Supporting Information for:

Excitonic Effects in Emerging Photovoltaic Materials: A Case Study in Cu_2O

Stefan T. Omelchenko[†§], *Yulia Tolstova*[†], *Harry A. Atwater*[†§‖], *Nathan S. Lewis*[*‡§‖⊥]

[†]Division of Engineering and Applied Sciences, California Institute of Technology, Pasadena, CA 91125
[‡]Division of Chemistry and Chemical Engineering, California Institute of Technology, Pasadena, CA 91125
[§]The Joint Center for Artificial Photosynthesis, California Institute of Technology, Pasadena, CA 91125
[‖]Kavli Nanoscience Institute, California Institute of Technology, Pasadena, CA 91125
[⊥]Beckman Institute, California Institute of Technology, Pasadena, CA 91125

*Corresponding Author: nslewis@caltech.edu

This is a 15 page document with 7 sections (Experimental Methods, S1, S2, S3, S4, S5, S6) and 4 figures (S1-S4)

Experimental Methods

Substrate Growth:

Cuprous oxide substrates were grown by two methods. For photoluminescence measurements, single crystalline Cu_2O wafers were prepared by the floating zone technique. Feed and seed rods were grown by the thermal oxidation of high-purity Cu rods (Alfa Aesar, 99.999%) in a vertical tube furnace (Crystal Systems Inc.) in air for 100 h at 1050 °C. The rods were then cooled in N_2 at 120 °C/h. Prior to growth, the rods were cleaned in acetone and etched using dilute nitric acid (0.1 M) for 60 seconds. The rods were suspended by either Cu or Pt wire. Single crystals were grown in an optical floating zone furnace (CSI FZ-T-4000-H-VII-VPO-PC). Crystals were grown in air with the seed and feed rods counter-rotating at 7 rpm. The resulting single crystalline boules were diced into wafers along the growth axis and mechanically polished to a specular finish using diamond grit.

Polycrystalline Cu_2O substrates were grown for solar cell fabrication. High-purity Cu foil (Alfa Aesar, 99.9999%, 0.5 mm thick) was heated in a quartz tube under N_2(g) to 1025 °C at 1000 °C/h. The foils were then oxidized in air for 24 h and cooled under N_2(g) to room temperature. The resulting substrates were ~ 0.8 mm thick and had carrier concentrations ~10^{13} cm^{-3}.

Solar Cell Fabrication:

The photovoltaic device in this work was fabricated on a ~ 0.8 mm thick Cu_2O wafer grown by thermal oxidation of copper foil. The grain size of wafers grown by this process is typically of the order of several millimeters and in some cases almost the size of the entire wafer (~1 cm^2). The photovoltaic cells in this study were fabricated using a circular shadow mask

resulting in an ultimate cell size ~0.02 cm^2 so that individual solar cells were generally isolated to only 1 or 2 grains.

Prior to fabrication, the polycrystalline Cu_2O substrates were cleaned with isopropanol and loaded into a magnetron sputtering system with a base pressure of $1.7x10^{-7}$ Torr. The Cu_2O wafers were heated in vacuum for 90 min at 100 °C. A 45 nm layer of Zn(O,S) was co-sputtered from ZnO and ZnS targets at a working pressure of 5 mTorr Ar. The power on the ZnO target was 100W and the power on the ZnS target was 85W. After deposition, the samples were cooled to room temperature in vacuum and removed from the chamber. A shadow mask was placed over the samples and a 60 nm ITO layer was sputtered at 50 W in an Ar atmosphere with a working pressure of 3 mTorr at room temperature. A 100 nm Au back-contact was then sputter deposited on the back of the sample.

Characterization:

A Ti:sapphire laser (Libra, Coherent Inc.) with a fundamental 800 nm laser pulse, 120 fs pulse width, and 10 kHz repetition rate was used to pump an optical parametric amplifier (Opera Solo, Coherent Inc.) and generate visible light. Single crystalline Cu_2O wafers grown by the float-zone method were illuminated with wavelengths ranging from 400 to 550 nm. The time-averaged photoluminescence spectra were collected using a time-correlated single-photon-counting method using a streak camera (Hamamatsu Inc.) with 20 ps time resolution. The spectral response measurements were performed using a Xe arc lamp and slit monochromator (Newport Inc.), and a calibrated reference Si photodiode (Thor Labs Inc.) with a known spectral responsivity.

S1. Device Model and Model Parameters for Cu_2O

The Cu_2O-based photovoltaic was modeled as a simplified p-n^+ solar cell, using the following assumptions adopted by Ref. 1: (1) the depletion approximation; (2) the drift and diffusion currents are opposite and equal in magnitude within the depletion region; (3) recombination is neglected in the depletion region; (4) the solar cell is operating in low-level injection; (5) in the bulk, minority carriers flow by diffusion. The inclusion of excitons requires the modification of the "free carrier" model to include an additional term that accounts for the exchange between the excitons and free-carrier populations. In this case, the excess minority- carrier (Δn_e) and excess exciton (Δn_x) concentrations are governed by the following coupled differential equations:

$$D_e \frac{d^2\Delta n_e}{dz^2} = \frac{\Delta n_e}{\tau_e} - G_e e^{-\alpha z} + b(\Delta n_e N_A - \Delta n_x n^*) \quad (1)$$

$$D_x \frac{d^2\Delta n_x}{dz^2} = \frac{\Delta n_x}{\tau_x} - G_x e^{-\alpha z} - b(\Delta n_e N_A - \Delta n_x n^*) \quad (2)$$

where D is the diffusion coefficient, τ is the lifetime, and G is the wavelength-dependent generation rate.[1] The subscripts e and x refer to electrons and excitons, respectively. The third term in Equation S1 and S2 is the net rate at which electrons and holes bind to form excitons, and is derived from the law of mass action, where b is the coefficient for binding free carriers into excitons, N_A is the p-type doping density and n^* is the equilibrium constant for the exchange between excitons and free carriers (in equilibrium $n^* n_x = n_e n_h$). Further, free carriers and excitons were assumed to be in quasi-equilibrium at the edge of the depletion region. The coupled differential equations yield analytical solutions for the dark saturation current density, J_0, and the short-circuit current density, J_{sc},:

$$J_0 = eD_e n_0 \left(\frac{\gamma}{L_1} + \frac{1-\gamma}{L_2}\right) + eD_x n_x^0 \left(\frac{\zeta}{L_1} + \frac{1-\zeta}{L_2}\right) \quad (3)$$

$$J_{sc} = eG_e \left(\frac{\gamma}{\alpha + L_1^{-1}} + \frac{1-\gamma}{\alpha + L_2^{-2}}\right) + eG_x \left(\frac{\zeta}{\alpha + L_1^{-1}} + \frac{1-\zeta}{\alpha + L_2^{-2}}\right) \quad (4)$$

where e is the fundamental unsigned charge on an electron; n_0 and the n_x^0 are the equilibrium concentrations of electrons and excitons, respectively; and α is the wavelength-dependent absorption coefficient.[2] Additionally:

$$\gamma = \frac{1}{2} - \frac{M_\Delta + \frac{2M_{21}D_x}{D_e}}{2\sqrt{\delta}} \quad (5)$$

$$\zeta = \frac{1}{2} + \frac{M_\Delta - \frac{2M_{12}D_e}{D_x}}{2\sqrt{\delta}} \quad (6)$$

$$L_1 = \frac{1}{\sqrt{\varepsilon_1}} \quad (7)$$

$$L_2 = \frac{1}{\sqrt{\varepsilon_2}} \tag{8}$$

$$\varepsilon_1 = \frac{1}{2}(M_{11} + M_{22} - \sqrt{\delta}) \tag{9}$$

$$\varepsilon_2 = \frac{1}{2}(M_{11} + M_{22} + \sqrt{\delta}) \tag{10}$$

$$M_\Delta = M_{11} - M_{22} \tag{11}$$

$$\delta = M_\Delta^2 + 4M_{12}M_{21} \tag{12}$$

$$M_{11} = \left(\frac{1}{\tau_e} + bN_A\right)\frac{1}{D_e} \tag{13}$$

$$M_{22} = \left(\frac{1}{\tau_e} + bn^*\right)\frac{1}{D_x} \tag{14}$$

$$M_{12} = -\frac{bn^*}{D_e} \tag{15}$$

$$M_{21} = -\frac{bN_A}{D_x} \tag{16}$$

The "free carrier" solutions for the dark saturation and short-circuit current densities, respectively, for an p-n^+ solar cell are given by:

$$J_{0,FC} = -\frac{eD_e\Delta n_0}{L_e} \tag{17}$$

$$J_{sc,FC} = \frac{eG_e}{\alpha + L_e^{-1}} \tag{18}$$

Equation S17 and S18 were used to compare the performance of the excitonic model to that of the traditional "free carrier" model. The major effect of excitons, effecting a coupling between the electron and hole population and exciton population, alters the diffusion characteristics of both free carriers and excitons, as can be seen from Equation S3-S4 and S17-S18. Thus, a fraction γ of photogenerated electrons move with a diffusion length L_1 and the remaining photogenerated electrons (1-γ) diffuse with a diffusion length L_2, where L_1 and L_2 are effective diffusion lengths that account for the interactions between the exciton and free carrier populations. Similarly, a portion of photogenerated excitons ζ and the remaining exciton fraction (1-ζ) have diffusion lengths L_1 and L_2, respectively.

Equation S3 and S4 are fundamentally dependent on the experimentally measured parameters D and τ, which are affected by temperature and doping density. The performance of the p-n^+ Cu_2O solar cell can then be evaluated a function of temperature and N_A. The dependence of the exciton binding energy on doping density can be estimated assuming that the exciton binding energy falls off to zero as the doping density approaches the Mott density:

$$E_x = E_{x\infty}\left[1 - \sqrt{\frac{N_A}{n_{Mott}}}\right]^2 \quad (19)$$

where $E_{x\infty}$ is the unscreened exciton binding energy, 150 meV in Cu_2O.[3-4] The Mott density was estimated using the value for Si as a function of temperature:

$$n_{Mott} = 10^{16}\,\frac{a_B^{Si}}{a_B^{Cu_2O}}\,\frac{\varepsilon^{Si}}{\varepsilon^{Cu_2O}}\,T \quad (20)$$

where a_B is the exciton Bohr radius and ε is the dielectric constant. The superscripts Si and Cu_2O refer to silicon and Cu_2O, respectively. The unscreened exciton binding energy is assumed to be independent of temperature.

The electronic band gap E_g of Cu_2O was measured down to 4 K using the threshold energy of the free exciton peak in the photoluminescence spectrum. The temperature dependence of E_g was fit using an oscillator model that accounts for exciton-phonon coupling:

$$E_g(T) = E_g(0) + S\hbar\omega - S\hbar\omega \coth\left(\frac{\hbar\omega}{2k_BT}\right) \quad (21)$$

where $E_g(0) = 2.173$ eV is the electronic band gap at $T = 0$ K, $S = 1.89$ is a material specific constant, and $\hbar\omega = 13.6$ meV is the phonon energy of the phonon (Γ_{12}^-) emitted during exciton luminescence.[5]

The electron mobility was estimated from majority-carrier data in literature. The effect of temperature and doping density on the majority carrier mobility was estimated as:

$$\frac{1}{\mu_h} = \frac{1}{\mu_T} + \frac{1}{\mu_I} \quad (22)$$

where

$$\mu_T = 8511 \times 10^{-0.00643T} \quad (23)$$

is the mobility caused by lattice vibrations, with the value determined from as-grown Cu_2O crystals.[6-7] Empirical data for the mobility as a function of hole concentration due to Na doping was used as an interpolating function in the model for μ_I.[8]

The minority-carrier lifetime is an important materials property that plays a significant role in determining the performance of solar cells in the free carrier model. Generally, the electron lifetime is estimated from the electron diffusion length fit from the external quantum efficiency, and varies from ~100 ns for undoped samples to on the order of ~ 1 ns for doped samples.[9-10] As such, we have estimated the electron lifetime as:

$$\tau_e = \frac{100}{1+10^{-16}\,N_A} \quad (24)$$

The lowest lying exciton states in Cu_2O are the spin singlet "paraexciton" and spin triplet "orthoexciton", which are split by a spin exchange, with the paraexciton lying 12 meV lower than the orthoexciton. The paraexciton transition is dipole- and quadrupole-forbidden, and the

transition is dipole-forbidden for the orthoexciton due to inversion symmetry of the Cu_2O crystal. This behavior leads to long-lived exciton states; the paraexciton lifetime, for example, has been measured to be > 14 μs at low temperatures.[11] The small energetic splitting between the two states causes the orthoexciton to decay into the paraexciton state on the picosecond time scale, while paraexcitons up-convert to orthoexcitons at the same rate.[12-13] Consequently, for temperatures relevant to photovoltaic operation, the ortho- and paraexciton lifetimes are the same, given by the most rapid recombination pathway. Thus, the temperature-dependent orthoexciton lifetime data from Ref. [14] was used for τ_x (implemented as an interpolating function in our code), assuming that the exciton lifetime is < 1μs.[14]

The mean time for excitons to form is given by $\tau_b = \frac{1}{bn^*}$, where n^* is found by treating the exciton and electron-hole system as an ideal gas mixture and neglecting exciton-exciton interactions:

$$n^* = \frac{n_{0e}n_{0h}}{n_{0x}} T^{3/2} e^{-E_x/k_B T} \tag{25}$$

with the density of states,

$$n_{0i} = \frac{g_i(2\pi m_i k_B)^{3/2}}{h^3} \tag{26}$$

where g_i is the degeneracy term, m_i is the translational mass and h is Planck's constant. For Cu_2O $g_e = 2, g_h = 2$ and $g_x = g_e g_h = 4$ and $m_e = 0.99m_0, m_h = 0.58m_0$, and $m_x = 3.0m_0$, where m_0 is the fundamental electron mass. The exciton binding coefficient b has not been measured in Cu_2O, so we have used the variation of b with temperature for Si:

$$b = 10^{-3}T^{-2} + 2.5 \times 10^{-6}T^{-1/2} + 1.5 \times 10^{-7} \tag{27}$$

in units of $cm^3 \cdot s^{-1}$.[15] This is likely an underestimation of b in Cu_2O, because the exciton binding energy in Cu_2O is approximately an order of magnitude larger than that in Si.

S2. Effect of Excitons on Diffusion Length

The diffusion lengths of electrons and excitons were calculated by use of:

$$L_e = \sqrt{D_e \tau_e} \tag{28}$$

$$L_x = \sqrt{D_x \tau_x} \tag{29}$$

The diffusion coefficient of electrons in Cu_2O has yet to be measured, so D_e was estimated using the Einstein relation:

$$D_e = \frac{1}{e}\frac{m_h}{m_e}\mu_h k_B T \tag{30}$$

where the electron mobility was estimated by weighting the hole mobility by the ratio of the electron and hole translational masses. This approach yields values of ~2 μm for L_e, which agrees well with measured values from the literature.[9-10, 16-17] Similarly, the exciton diffusion length was calculated using:

$$D_x = \mu_x k_B T \tag{31}$$

The exciton mobility μ_x has been measured accurately down to low temperatures. Above 10 K, the following expression was found to be in good accord with the experimentally measured exciton mobility:

$$\mu_x = \frac{2\sqrt{2\pi}\hbar^4 \rho v_l^2}{3\mathcal{D}^2 m_x^{5/2}} (k_B T)^{-3/2} \tag{32}$$

where, $\rho = 6.11$ g·cm^{-3} is the mass density of the Cu_2O crystal, $v_l = 4.5 \times 10^5$ m·s^{-1} is the thermal velocity, and $\mathcal{D} = 1.2$ is the deformation potential.[18]

The principal effect of excitons on solar cell performance is to modify the diffusion characteristics of photogenerated species by effectively coupling the motion of free carriers and excitons.[1-2] Figure S1 shows the effect of temperature and doping density on the diffusion lengths L_e, L_x, L_1, and L_2. The exciton diffusion length is approximately constant with temperature, and is almost an order of magnitude greater than L_e, which varies significantly with temperature. For low-to intermediate doping densities, this behavior causes L_1 to approach L_e, especially at high temperatures. At low temperatures, where excitons dominate, L_1 tends towards L_x. L_2 is substantially lower than L_1 for all temperatures.

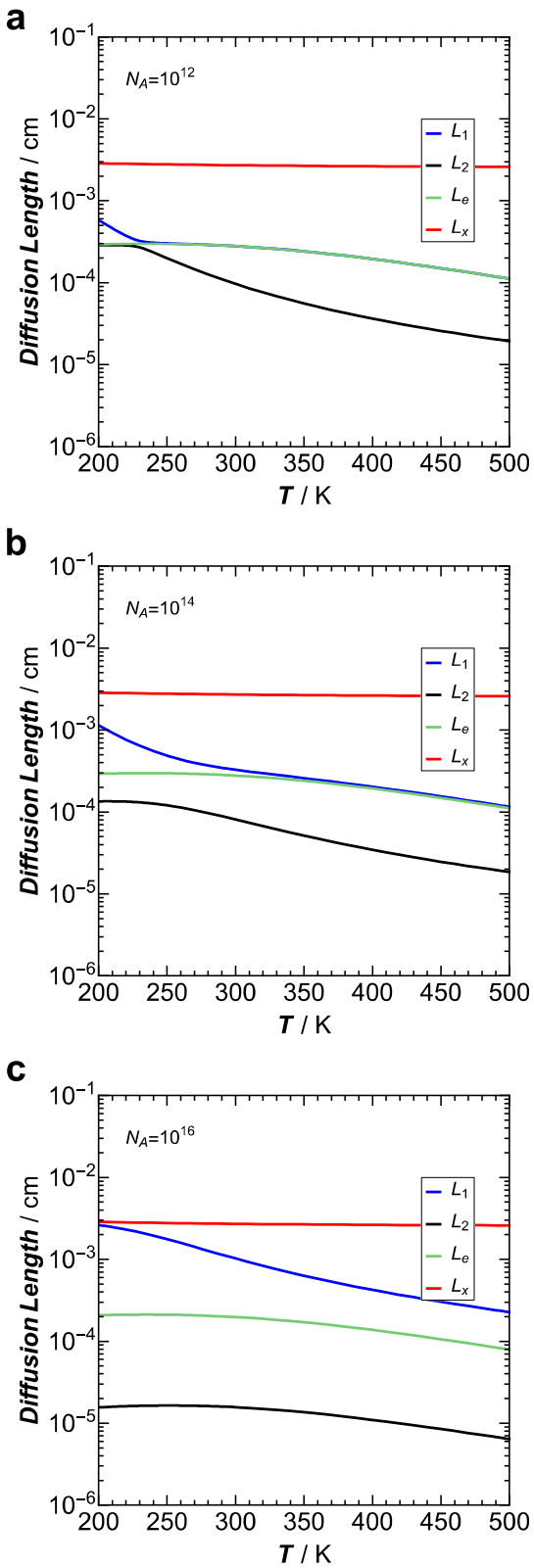

Figure S1. The simulated electron, exciton and effective diffusion lengths for Cu_2O for doping densities a) 10^{12}, b) 10^{14}, and c) 10^{16}.

S3. Equilibrium concentration of excitons and free carriers for calculation of J_0

A fundamental assumption in our model is that excitons and free carriers are in equilibrium in the Cu_2O bulk up to the edge of the depletion region, such that:

$$n_i^2 = n_0 p_0 = n_x^0 n^* \tag{33}$$

where, n_0, p_0, and n^0_x are the electron, hole concentrations, respectively. Here, we assume that the hole concentration is given by the ionized dopant density N_A and thus, in equilibrium, the ratio of excitons to free electrons is given by:

$$\frac{n_x^0}{n_0} = \frac{N_A}{n^*} \tag{34}$$

The equilibrium exciton ratio is shown in **Figure S2**. As expected, the excitonic fraction of the photogenerated population increases with decreasing temperature and increasing doping density. The exciton density is greater than the free carrier population at room temperature for large doping densities. From, Equation S32 and S33 the equilibrium exciton concentration is given by:

$$n_x^0 = \frac{n_i^2}{n^*} \tag{35}$$

and the equilibrium electron concentration is given by the typical expression:

$$n_0 = \frac{n_i^2}{N_A} \tag{36}$$

The intrinsic carrier concentration can be calculated from the effective density of states in the valence and conduction bands, respectively:

$$N_C(T) = 2\left(\frac{2\pi m_e k_B T}{h^2}\right)^{\frac{3}{2}} = 4.75 \times 10^{15} T^{3/2} \tag{37}$$

$$N_V(T) = 2\left(\frac{2\pi m_h k_B T}{h^2}\right)^{\frac{3}{2}} = 2.14 \times 10^{15} T^{3/2} \tag{38}$$

$$n_i^2(T) = N_C N_V e^{-\frac{E_g(T)}{k_B T}} = 1.014 \times 10^{31} T^{3/2} \tag{39}$$

in cm^{-3}.[19] Using these values and the parameters outlined above, the dark saturation current density J_0 can be calculated.

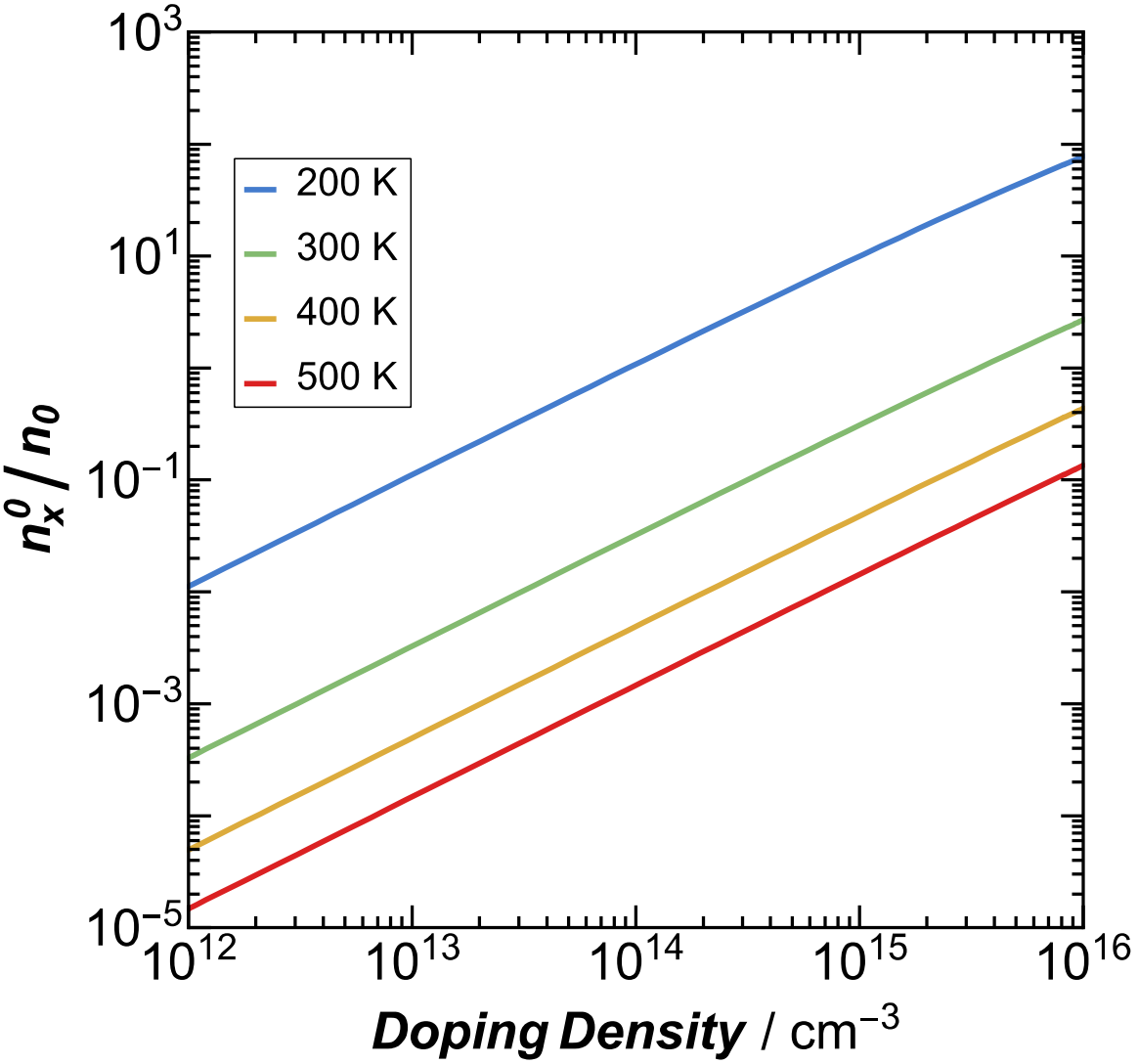

Figure S2: The equilibrium ratio of excitons to free carriers as a function of doping density for temperatures ranging from 200 to 500 K.

S4. Absorption, generation and calculation of J_{sc}

The calculation of J_{sc} requires knowledge of the generation rate of excitons and free carriers, as well as the absorption coefficient in the visible spectrum. We have calculated J_{sc} using the full wavelength dependence of G_e and α. The experimentally determined absorption coefficient was used, and the absorption coefficient of Cu_2O was assumed to not vary substantially over the temperature range evaluated in this study (200 – 500 K).[20] The wavelength-dependent electron and exciton generation rate were estimated by:

$$G(\lambda) = \alpha(\lambda)\Phi(\lambda) \tag{40}$$

where Φ is the photon flux from the global AM 1.5 solar spectrum. To differentiate between exciton and free carrier generation, the free carriers were assumed to be generated for absorption of a photon with energy above the electronic band gap, and excitons were assumed to be generated only in the case for photon excitation with an energy between the electronic band gap and the excitonic band edge (E_g-E_x). Thus, the short-circuit current density is the summation of two parts, one free-carrier and one excitonic:

$$J_{sc} = e\int_{E_g}^{\infty} \alpha(\lambda)\Phi(\lambda)\left(\frac{\eta}{\alpha(\lambda)+L_1^{-1}}+\frac{1-\eta}{\alpha(\lambda)+L_2^{-2}}\right)d\lambda + e\int_{E_g-E_x}^{E_g} \alpha(\lambda)\Phi(\lambda)\left(\frac{\zeta}{\alpha(\lambda)+L_1^{-1}}+\frac{1-\zeta}{\alpha(\lambda)+L_2^{-2}}\right)d\lambda \quad (41)$$

This approach is an oversimplification, as we have demonstrated experimentally in the main text. Even above-band-gap illumination leads to excitonic generation that is observable as a free-exciton peak in the photoluminescence spectrum.

S5. Fill Factor and Efficiency

The current density and voltage at the maximum power point, J_{mpp} and V_{mpp}, were determined by generating an *J-V* characteristic by numerically solving Equation 1 for an array of voltages. The fill factor (*FF*) was then calculated using the formula:

$$FF = \frac{J_{mpp}V_{mpp}}{J_{sc}V_{oc}} \quad (42)$$

and the efficiency (η) is then given by:

$$\eta = \frac{V_{oc}\,J_{sc}\,FF}{P_{in}} \quad (43)$$

where P_{in} is the power incident on the Cu_2O cell, in this case, the standard AM 1.5 solar spectrum. The *FF* is depicted in **Figure S3**. The fill factors were in close agreement between the excitonic and FC models, except for the highest doping density.

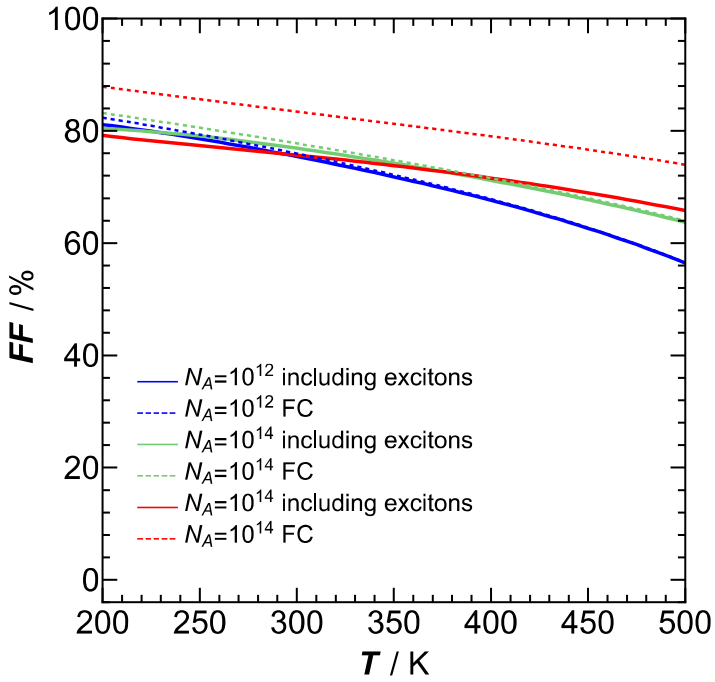

Figure S3: The simulated fill-factor for the excitonic and FC models. The fill factors were in close agreement except at the highest doping densities, where large enhancement in the J_{sc} dominates and leads to an increase in the solar-cell efficiency relative to the FC case.
References

S6. Characteristics of Polycrystalline Cu_2O wafers

Room temperature photoluminescence spectra were also collected for the polycrystalline Cu_2O wafers grown by thermal oxidation, which were used in device fabrication. The spectra were collected using a 514 nm excitation for powers ranging from 85 μW to 5.4 mW. The photoluminescence spectrum near the orthoexciton luminescence peak is shown in Figure S4. The unusual peak shape is due to the convolution of the orthoexciton peak and the phonon-assisted exciton peak, which broadens and grows at higher temperatures where the absorption probability of phonons by excitons is large.[5, 21-22] The peak was evident even at the lowest of excitation powers (0.85 μW). Thus, excitons are generated under visible excitation even in polycrystalline Cu_2O substrates used in photovoltaic fabrication.

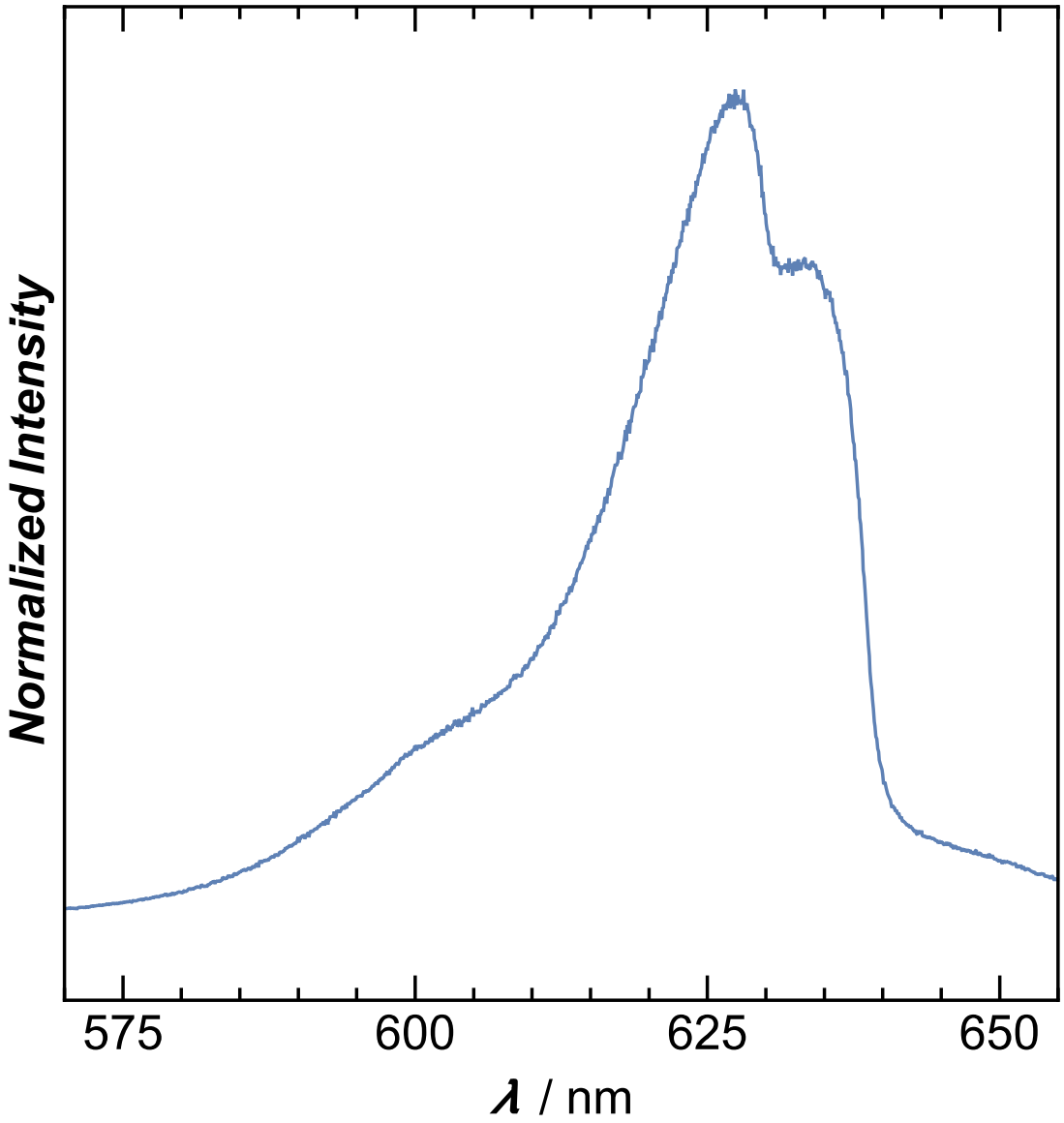

Figure S4: Photoluminescence spectrum of the free exciton peak in thermally oxidized, polycrystalline Cu_2O wafers at room temperature using a 2.4 mW, 514 nm excitation.

References

1. Corkish, R.; Chan, D. S. P.; Green, M. A., Excitons in silicon diodes and solar cells: A three-particle theory. *Journal of Applied Physics* **1996,** *79* (1), 195-203.
2. Zhang, Y.; Mascarenhas, A.; Deb, S., Effects of excitons on solar cells. *Journal of Applied Physics* **1998,** *84* (7), 3966-3971.
3. Kane, D. E.; Swanson, R. M., The effect of excitons on apparent band gap narrowing and transport in semiconductors. *Journal of Applied Physics* **1993,** *73* (3), 1193-1197.

4. Moskalenko, S. A.; Snoke, D. W., *Bose-Einstein Condensation of Excitons and Biexcitons and Coherent Nonlinear Optics with Excitons*. Cambridge University Press: New York, New York, 2000.
5. Ito, T.; Masumi, T., Detailed Examination of Relaxation Processes of Excitons in Photoluminescence Spectra of Cu_2O. *Journal of the Physical Society of Japan* **1997,** *66* (7), 2185-2193.
6. Shimada, H.; Masumi, T., Hall Mobility of Positive Holes in Cu_2O. *Journal of the Physical Society of Japan* **1989,** *58* (5), 1717-1724.
7. Biccari, F. Defects and Doping in Cu_2O. Universita di Roma, 2009.
8. Minami, T.; Nishi, Y.; Miyata, T., Impact of incorporating sodium into polycrystalline p-type Cu_2O for heterojunction solar cell applications. *Applied Physics Letters* **2014,** *105* (21), 212104.
9. Xiang, C.; Kimball, G. M.; Grimm, R. L.; Brunschwig, B. S.; Atwater, H. A.; Lewis, N. S., 820 mV open-circuit voltages from Cu_2O/CH3CN junctions. *Energy & Environmental Science* **2011,** *4* (4), 1311-1318.
10. Biccari, F.; Malerba, C.; Mittiga, A., Chlorine doping of Cu_2O. *Solar Energy Materials and Solar Cells* **2010,** *94* (11), 1947-1952.
11. Mysyrowicz, A.; Hulin, D.; Antonetti, A., Long Exciton Lifetime in Cu_2O. *Physical Review Letters* **1979,** *43* (15), 1123-1126.
12. Snoke, D. W.; Shields, A. J.; Cardona, M., Phonon-absorption recombination luminescence of room-temperature excitons in Cu${}_{2}$O. *Physical Review B* **1992,** *45* (20), 11693-11697.
13. Snoke, D. W.; Lin, J. L.; Wolfe, J. P., Coexistence of Bose-Einstein paraexcitons with Maxwell-Boltzmann orthoexcitons in Cu_2O. *Physical Review B* **1991,** *43* (1), 1226-1228.
14. Koirala, S.; Naka, N.; Tanaka, K., Correlated lifetimes of free paraexcitons and excitons trapped at oxygen vacancies in cuprous oxide. *Journal of Luminescence* **2013,** *134*, 524-527.
15. Nolle, E., Recombination Through Exciton States in Semiconductors. *Soviet Physics - Solid State* **1967,** *9* (1), 90-94.
16. Trivich, D.; Wang, E. Y.; Komp, R. J.; Weng, K.; Kakar, A., Cuprous oxide photovoltaic cells. *Journal of the Electrochemical Society* **1977,** *124* (8), C318.
17. Olsen, L. C.; Addis, F. W.; Miller, W., Experimental and theoretical studies of Cu_2O solar cells. *Solar Cells* **1982,** *7* (3), 247-279.
18. Trauernicht, D. P.; Wolfe, J. P., Drift and diffusion of paraexcitons in Cu_2O: Deformation-potential scattering in the low-temperature regime. *Physical Review B* **1986,** *33* (12), 8506-8521.
19. Sze, S. M.; Ng, K. K., *Physics of semiconductor devices*. 3rd ed.; Wiley-Interscience: Hoboken, N.J., 2007; p x, 815 p.
20. Malerba, C.; Biccari, F.; Leonor Azanza Ricardo, C.; D'Incau, M.; Scardi, P.; Mittiga, A., Absorption coefficient of bulk and thin film Cu_2O. *Solar Energy Materials and Solar Cells* **2011,** *95* (10), 2848-2854.
21. Petroff, Y.; Yu, P. Y.; Shen, Y. R., Luminescence of Cu_2O-Excitonic Molecules, or Not? *Physical Review Letters* **1972,** *29* (23), 1558-1562.
22. Petroff, Y.; Yu, P. Y.; Shen, Y. R., Study of photoluminescence in Cu_2O. *Physical Review B* **1975,** *12* (6), 2488-2495.